Photoresponsive synthetic receptors: binding properties and photocontrol of catalytic activity

Frank Würthner and Julius Rebek, Jr.*
Department of Chemistry, Massachusetts Institute of Technology, Cambridge, Massachusetts 02139, USA

The photoresponsive ditopic receptors **1a,b** bearing two adenine binding sites linked by an azobenzene moiety were prepared. Photochromism, binding of mono- and bis-adenine derivatives and template effects on the coupling reaction of aminoadenosine **2** and the adenosine-derived active ester **3** were studied. Photoswitching of the azobenzene linker from the extended *E* to the folded *Z* isomer enhances the catalytic activity of the template **1a** by a factor of 50. The binding studies provide evidence for the formation of termolecular complexes **1·2·3** and allow for mechanistic considerations. The influence of various adenine derivatives on the rate of the thermal *Z* ⟶ *E* isomerization of (*Z*)-**1a,b** was evaluated and a significant stabilization of the *Z* isomers by the bis-adenine guest **4** was observed.

Within the last years we have witnessed a change in the focus of supramolecular chemistry to depart from purely structural aspects to dynamics and functionality.[1] Specifically, the events of molecular recognition have been used to create carriers for selective *transport*,[2] to obtain *sensors* for guest molecules,[3] and to *transform* substrates into products by template effects.[4] Other work has focused on *controlling* molecular recognition by means of external signals such as light or voltage.[5] However, these studies have also confirmed that, in spite of the abundance of high-performance functional units for specific single operations, complex functions are still difficult to achieve. Thus, all of the examples cited above are limited to just *two* functional components and the efficacy falls far behind that of biological systems. On the other hand, synthetic systems exhibit the advantage of much smaller size, their specific functions are much easier to study and chemistry offers a means to optimize a promising supramolecular structure.

In this paper we report our results on a receptor system which involves *three* functional features, that are *recognition*, *reactivity* and *control* by photoswitching.[6] The intended interaction of these components is to give a supramolecular catalytic entity that mimics the basic features of rhodopsin, the biological phototrigger in vision. In this process light irradiation causes a *cis* ⟶ *trans* isomerization of retinal that induces a conformational change in the conjugated protein. The change of molecular shape then triggers a chemical reaction that initiates an enzymatic cascade ultimately leading to a neural response.[7]

Fig. 1 depicts the three basic functionalities required to achieve such a performance. Two binding units allow for substrate recognition, a switchable unit enables change of the molecular shape by an external stimulus (light) and a reactive function effects transformation.

To elaborate such a system we started with highly efficient carbazole-based receptors for adenines (Scheme 1).[8] The receptor–adenine recognition event relies on simultaneous Watson–Crick and Hoogsteen base pairing between the two imides and the purine nucleus as well as π-stacking of the two aromatic surfaces. This tritopic chelation not only produces high binding affinities in organic solvents but also a well defined geometry of the complex. Recently two of these receptors were connected by spacers to give templates which are able to increase the rate of the coupling reaction between 5′-amino-5′-deoxy-2′,3′-*O*-isopropylideneadenosine (**2**) and *p*-nitrophenyl (PNP) ester **3** to give amide **4** (Scheme 2).[9a] By variation of the spacer unit geometrical factors (shape, distance and rigidity) could be elucidated, which are important to obtain highly efficient template molecules.[9b,c]

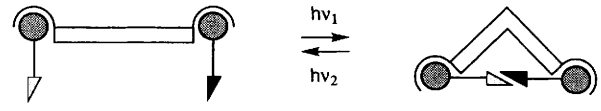

Fig. 1 Schematic illustration of a photoswitchable template catalyst

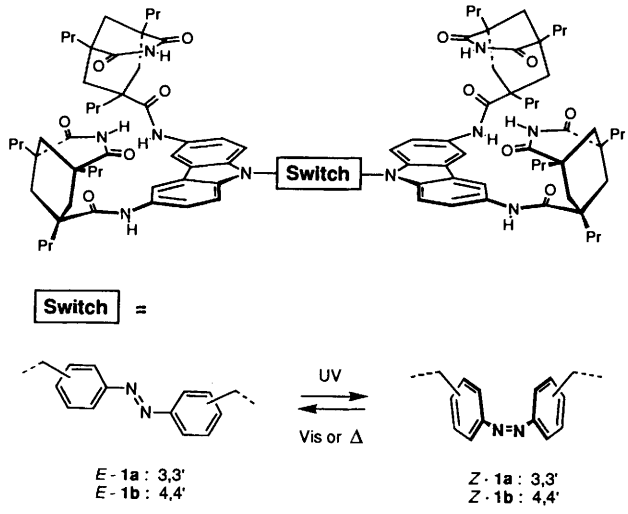

Scheme 1 Photoswitchable synthetic receptors **1a,b**

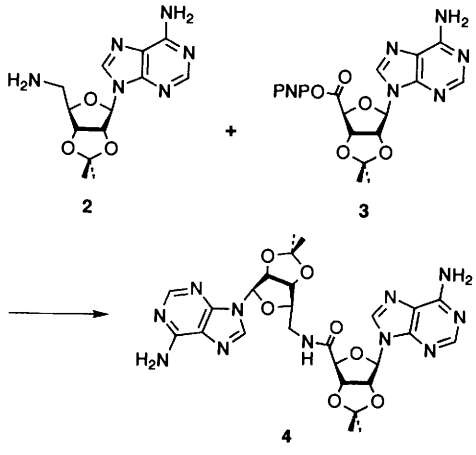

Scheme 2

Table 1 E/Z ratios of receptors **1a,b** and reference compounds **9a,b** in their thermal and photostationary equilibria in chloroform[a]

	1a	1b	9a	9b
Δ[b]	100/0	100/0	100/0	100/0
VIS[c]	70/30	75/25	75/25	75/25
UV[d]	50/50	50/50	10/90	6/94

[a] Determined by ^{1}H NMR spectroscopy, error ±3%. [b] Thermal equilibrium. [c] Irradiation with a tungsten lamp. [d] Irradiation with UV light at 366 nm.

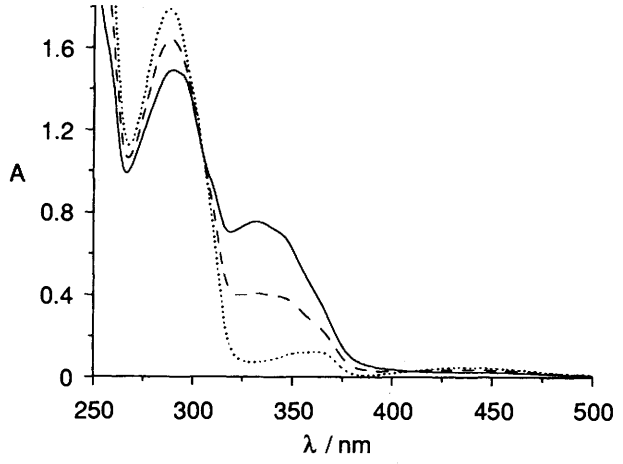

Fig. 2 Electronic absorption spectra of receptor (*E*)-**1b** (——), (*E*)/(*Z*)-**1b** in the photostationary state at 366 nm (— —) and calculated (*Z*)-**1b** (· · ·) in chloroform (c = 0.05 mol dm^{-3})

To control the rate of the amide bond formation between **2** and **3**, we had to introduce a 'spacer' unit which is responsive to light. The requirements for the photocontrolling unit were pronounced and reversible switchability, and a significant and predictable structural change that allows control of the distance and orientation of the template-coordinated reactants. For this purpose azobenzenes seemed to be well suited. Photoswitchability between the two isomeric E and Z species is highly reversible[10] and a significant magnitude of the structural change from the extended E to the folded Z isomer is confirmed by crystallographic data.[11] From CPK models and calculations[12] with various connecting units template molecules **1a,b** emerged, since only their Z forms are predicted to accommodate the reactants in a favourable geometry.

Receptors (*E*)-**1a,b** were readily assembled by alkylation of phthaloyl-protected diaminocarbazole **5** with bis(bromomethyl)azobenzenes (*E*)-**6a,b**,[13] followed by deprotection using methylamine and acylation with Kemp's imine acid chloride **8**[14] according to Scheme 3.

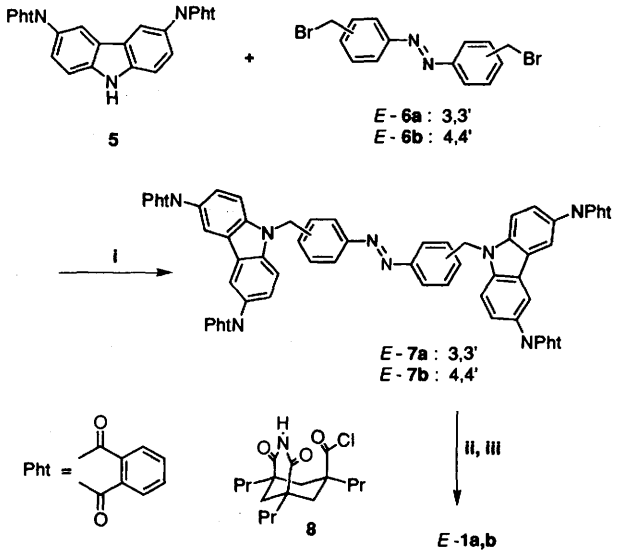

Scheme 3 Synthesis of receptors (*E*)-**1a,b**. Reagents and conditions: i, Bu^{t}OK, 18-crown-6, THF, room temp.; ii, methylamine, THF–MeOH, room temp.; iii, **8**, pyridine, reflux, exclusion of light.

Results and discussion

Photoswitching of receptors 1a,b

The photoactivity of the new receptor molecules **1a,b** was confirmed by irradiation of chloroform solutions with UV and visible light followed by ^{1}H NMR and UV–VIS analysis. Fig. 2 shows the absorption spectra of receptor **1b** as a pure E isomer and in its photostationary equilibrium obtained after irradiation with light of a wavelength of 366 nm. The isomeric composition of the receptors **1a,b** and of the model chromophores **9a,b**[15] in different photostationary equilibria are collected in Table 1.

Although switching is possible for all the compounds studied, it is quite obvious that $E \longrightarrow Z$ conversion at 366 nm is less efficient for the receptors **1a,b** than for the azobenzene model chromophores **9a,b**. To understand this result, the absorption

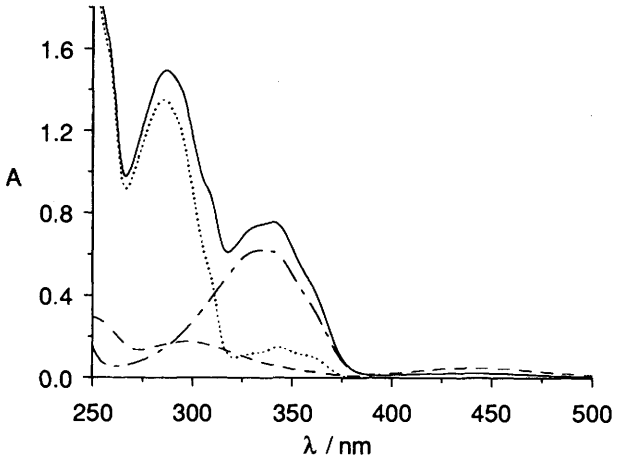

Fig. 3 Electronic absorption spectra of carbazole **10** (· · ·, c = 0.1 mmol dm^{-3}), azobenzene (*E*)-**9b** (– – –, c = 0.05 mmol dm^{-3}) and (*E*)/(*Z*)-**9b** in the photostationary state at 366 nm (— —, c = 0.05 mmol dm^{-3}) in chloroform, and calculated spectrum for (*E*)-**1b** (——, c = 0.05 mmol dm^{-3}), obtained by summation of the component spectra [2 × **10** + (*E*)-**9b**]

spectra of **9a,b** and **10** were recorded (Fig. 3) and the absorption spectra of the pure (*Z*)-**1a,b** were calculated (Fig. 2). Also included in Fig. 3 is the sum of these component spectra [two carbazole **10** and one (*E*)-azotoluene **9b**] to give a calculated spectrum of (*E*)-**1b**. The calculated spectrum gives an almost perfect match with the observed spectrum of compound (*E*)-**1b**. Therefore the electronic coupling between the carbazoles and the azobenzene subunit is weak and the individual chromophores keep their characteristic absorption properties. The absorption band between 250 and 300 nm is mainly attributed to the carbazole unit [**10**: λ = 286 nm, ε = 28 000 dm^3 mol^{-1} cm^{-1}]. Between 300 and 400 nm the strongest absorption comes from the (*E*)-azobenzene group [ε = 25 000 dm^3 mol^{-1} cm^{-1} at λ = 336 nm for (*E*)-**9b**], followed by a weak absorption of the carbazoles [ε = 2900 dm^3 mol^{-1} cm^{-1} at λ = 343 nm for **10**] and almost no absorption by (*Z*)-azobenzene. Finally, in the visible part of the spectrum only the azobenzene chromophores exhibit absorption bands [ε = 870 dm^3 mol^{-1} cm^{-1} at λ = 438 nm for (*E*)-**9b** and ε = 2030 dm^3 mol^{-1} cm^{-1} at λ = 440 nm, calculated for (*Z*)-**9b**].

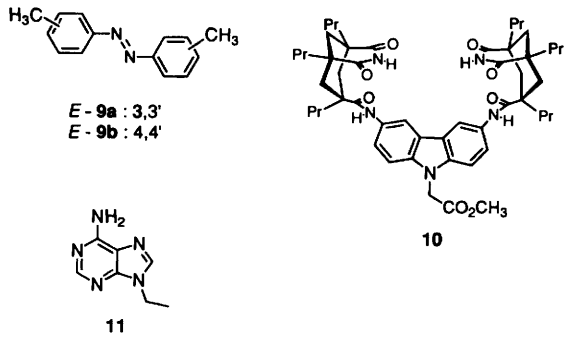

Scheme 4

Although the electronic coupling between the individual chromophores is rather weak and reversible *E*–*Z* conversion takes place under irradiation, there is a distinct influence of the carbazole subunit on the photostationary equilibrium at 366 nm, but not at wavelengths above 400 nm (VIS). A comparison of the remaining absorption band in the calculated spectrum of (*Z*)-**1b** in Fig. 2 with the absorption spectra of almost pure (*Z*)-**9b** and of carbazole **10** clearly indicates that the difference in the photostationary equilibria at 366 nm is caused by the absorption of the carbazole units. Whereas (*E*)-azobenzenes **9a,b** can be converted almost completely into the (*Z*)-azobenzenes, because the latter do not interact with light of this wavelength, receptors (*Z*)-**1a,b** are still excited because of the carbazole absorption band. This energy absorbed by the carbazole chromophore is transferred to the azobenzene unit and $Z \longrightarrow E$ conversion takes place.[16] Therefore the difference in the *E*/*Z* distributions of the azobenzenes **1a,b** and **9a,b** is explained by the absorption bands of the additional carbazole chromophores.

With respect to our envisaged goal of switchable template catalysis, it is important to note that a complete conversion into the *Z* isomer is not required, because the remaining *E* isomer is expected to have no catalytic activity. A conversion of 50% of the template molecules into the active *Z* form is therefore sufficient.

Binding of adenine guest molecules

To obtain highly efficient templates two basic requirements have to be met. First, high binding affinities between the template and the substrate molecules are essential. This means for the coupling reaction shown in Scheme 2 that a termolecular complex **1·2·3** has to form wherein each carbazole receptor site carries one adenine substrate molecule. Second, the template has to provide a favourable geometry to facilitate the bond formation process. Specifically, complementarity of the template to the transition state of the coupling reaction is desired. As the exact structure of the transition state is rarely known, however, template design is often based on efficient product binding, which can be studied by simple binding experiments.

The interaction between the mono-receptor **10** and various (mono-) adenines has been determined previously by ^{1}H NMR titration experiments,[8,9] According to these studies 1:1 complexes of high stability are formed in chloroform, which are based on chelation of adenines by the two imides attached to the carbazole surface by simultaneous Watson–Crick and Hoogsteen hydrogen bonding as well as π-stacking. Different substituents at N9 of adenine and at N9 of carbazole contribute only to a minor part (~1 kcal mol^{-1}) to the binding energy, probably *via* van der Waals interactions. However, by reexamining this system in a much more dilute solution by UV–VIS spectroscopy, we obtained some new insights into carbazole-based receptor molecules. A UV–VIS dilution study of receptor **10** at concentrations between 1×10^{-5} and 6×10^{-4} mol dm^{-3} is indicative of a two-state system (significant absorbance changes at 327 and 358 nm and two isosbestic points at 318 and 344 nm) and the fit to eqn. (1) is rather good

$$\mathbf{10} + \mathbf{10} \rightleftharpoons (\mathbf{10})_2 \quad K_a = \frac{[(\mathbf{10})_2]}{[\mathbf{10}]^2} \qquad (1)$$

giving a dimerization constant K_a of 3000 dm^3 mol^{-1} (4.7 ± 0.1 kcal mol^{-1} at a 95% confidence level). This value is rather high, but can be rationalized by molecular modelling by two carbazoles stacked in an *anti* orientation, which allows hydrogen bonding between the imides in pairs at each side of the dimer.

The amount of these dimers in solution is highly concentration dependent. At the concentration of 0.01 mmol dm^{-3} used in typical UV–VIS titrations (*vide infra*) only 5% of receptor molecules are dimerized. On the other hand, dimers dominate at higher concentrations, which are typical for NMR experiments, *e.g.*, 67% at 1 mmol dm^{-3}. Hence, these dimers also account for some of the peculiarities in previous NMR experiments in chloroform which show downfield shifted imide ^{1}H NMR signals at $\delta = 10.8$ (instead of 7.6 for a typical 'free' imide) and the appearance of broad signals for most of these receptor molecules. Despite these new findings in the properties of carbazole-based receptors, previous NMR results on adenine binding (5.6 kcal mol^{-1} for **10**/**11**)[8] are fairly well reproduced by UV–VIS titration experiments at 0.01 mmol dm^{-3} (Table 2). This shows that the binding constant between the carbazole-based receptors and the adenines is so high that the effect of receptor dimerization is negligible.

For the fully elaborated receptors (*E*)-**1a,b** UV–VIS dilution studies indicate a somewhat lower degree of self-association.† Presumably, the higher steric demand of the azobenzene unit at the carbazole nitrogen disfavours dimer formation. A careful evaluation, however was not possible because the relevant absorption change was superimposed by the strong absorbance of the azobenzene chromophore. Based on these results, we performed the binding studies in dilute host solutions of receptors (*E*)-**1a,b** by titrating with guests **4** and **11**.‡ The interaction of 9-ethyladenine (**11**) and receptors (*E*)-**1a,b** is taken to be a model for the termolecular complex formed at the beginning of the coupling experiment. The interaction of product **4** with receptor (*E*)-**1a,b** is a model for the end of the reaction. As the rate-determining step of the amide bond formation between **2** and **3** is assumed to be the breakdown of the tetrahedral intermediate,[9] the latter interaction probably also reflects the interaction with the transition state.

Fig. 4 shows the titration data for receptor **1a** with mono-adenine **11** and bis-adenine **4** obtained at 313 nm. At this wavelength binding of adenines exerts a significant influence on the absorption of the carbazole chromophore. At other wavelengths similar curves are obtained, but the absorbance changes are smaller. The initial slope of the binding isotherm is clearly steeper when (*E*)-**1a** is titrated with product **4** than with **11**, but the final change in absorbance ΔA is about the same. The former observation suggests stronger binding of **4** and the latter involvement of both receptor sites in the binding process. Therefore a 1:2 binding model is appropriate for the system (*E*)-**1a**/**11** and a 1:1 binding model is likely for the system (*E*)-**1a**/**4**. Evidence for 1:1 binding between (*E*)-**1a** and **4** is also obtained from the break in the curve at one equivalent guest

† Since we were not able to isolate pure *Z* isomers and the titration experiments of 1:1 *Z*/*E* mixtures did not provide valuable information, this part of the paper is limited to the results obtained for the *E* isomers.
‡ Neglect of dimers is justified under these conditions. No aggregation of guest molecules **4** and **11** is observed by dilution studies for the concentration range used in the UV titration experiments.

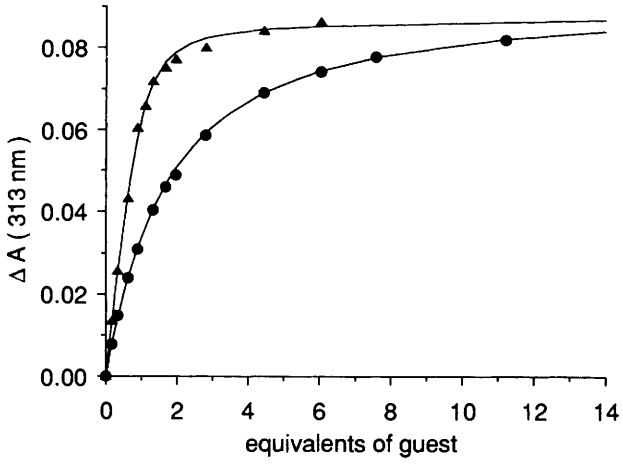

Fig. 4 Spectral data obtained by titration of receptor (*E*)-**1a** (c = 0.01 mmol dm^{-3} in chloroform) with mono-adenine **11** (●) and bis-adenine **4** (▲) and calculated lines. Equivalents of guest are defined assuming a 1 : 1 stoichiometry for (*E*)-**1a**/**4** and a 1 : 2 stoichiometry for (*E*)-**1a**/**11**.

Table 2 Association energy of receptors (*E*)-**1a,b** and **10** with adenine guest molecules **4** and **11** as determined by UV titration experiments at 313 nm[a]

Host	Guest	Stoichiometry[b]	$-\Delta G^{298}$/kcal mol^{-1}
10	**11**	1 : 1	6.0
(*E*)-**1a**	**11**	1 : 2	6.4, 5.8[c]
(*E*)-**1b**	**11**	1 : 2	6.4, 6.2[c]
(*E*)-**1a**	**4**	1 : 1	8.4
(*E*)-**1b**	**4**	1 : 1	7.5

[a] Experiments were performed twice. The uncertainties are less than 0.3 kcal mol^{-1} at the 95% confidence level. [b] The stoichiometry is an input into the calculation. The accuracy of the data does not always allow one to distinguish between the different models. Thus the choice of the model is based on chemical considerations and on the change in ΔA (see the text). [c] First and second binding event.

concentration (intersection of the two asymptotes). On the basis of these indications the titration data were evaluated for both receptors (*E*)-**1a,b** with both guest molecules **4** and **11** using non-linear least-squares regression analysis (Table 2).[17]

The evaluation of the spectral data for (*E*)-**1a,b**/**11** indicates two almost independent binding sites at (*E*)-**1a,b** with association energies in agreement with those obtained for the mono-receptor **10**. Note that when the sites are identical and when there is no interaction between the sites the first binding event is expected to have a four times higher binding constant than the second, which corresponds to a difference of 0.8 kcal mol^{-1}.[17a]

A more complicated situation is given in the titration of (*E*)-**1a,b**, with the bis-adenine reaction product **4**. Dimer formation or oligomerization (both 1 : 1) as well as a 1 : 2 or 2 : 1 stoichiometry is possible for this system and probably all occur and the composition of the mixture changes depending on the host : guest ratio. UV–VIS titration does not give much structural information, it only proves adenine binding to the carbazole surface by its impact on the π–π^* transitions. This effect is likely to be the same for all the species mentioned above. However, by combining structural information with the results of the titration studies some conclusions are possible. According to CPK models and force-field calculations the two adenines of **4** are not able to bridge the distance between the two receptor sites in the more extended receptor (*E*)-**1b**. As the final change in absorbance ΔA suggests involvement of both carbazole receptor sites in adenine binding, we can assume a 1 : 2 binding at higher concentration of **4**. The fact that the association energy is about 1 kcal mol^{-1} higher than that for **11** is attributed to additional

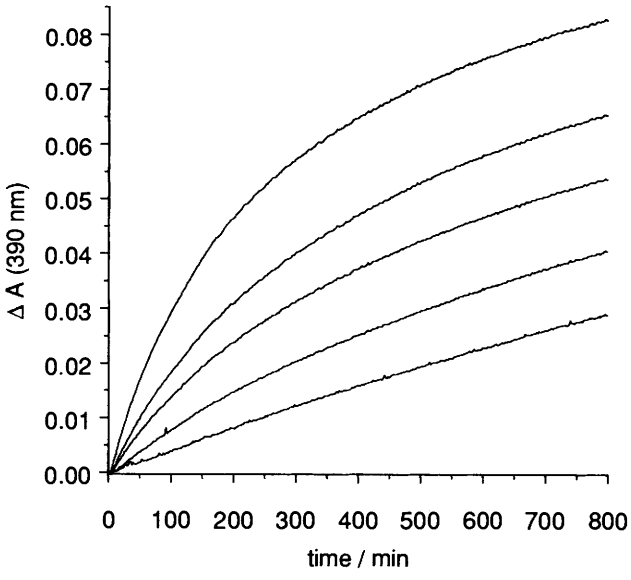

Fig. 5 Reaction of **2** and **3** in the presence of one equivalent of receptor **1a** at different *E*/*Z* ratios (100 : 0, 90 : 10, 80 : 20, 70 : 30, 50 : 50) monitored by UV–VIS spectroscopy

van der Waals contacts between **4** and (*E*)-**1b**, maybe by stacking of the two aromatic surfaces of the second adenine and the (*E*)-azobenzene unit. Similarly previous binding studies on monotopic carbazole-based receptors showed an increase of up to 1 kcal mol^{-1} for adenine nucleosides compared with simple ethyladenine **11**.[8]

In contrast, CPK models and calculations suggest that receptors (*E*)-**1a** can accommodate conformations in which the product **4** can interact with both receptor sites to form a 1 : 1 complex. Thus we assume here 1 : 1 binding at least for (*E*)-**1a**/**4** ratios higher than one (beginning of the titration experiment). Due to a lot of restricted rotations in such a 1 : 1 complex the gain in binding energy by the second binding event is small [~ 1 kcal mol^{-1}, compared with (*E*)-**1b**]. It seems therefore very likely that at higher concentration of **4** 1 : 2 complexes are also favoured for this receptor (*vide infra*).

Photoswitchable template effects

The receptors **1a,b** were designed to photocontrol the coupling reaction between **2** and **3**. As strong binding of the substrate molecules to all templates (*E*)-**1a,b** and (*Z*)-**1a,b** can be expected according to the previous section, geometrical factors are now of importance to make the difference. Whereas the *E* isomers of **1a,b** exhibit remote receptor sites, the *Z* isomers obtained by irradiation are folded and assumed to be more complementary to the species formed along the reaction coordinate. Therefore catalytic activity was expected only for the *Z* isomers.

The data in Table 3 and in Fig. 5 show that this is indeed the case. Specifically, irradiation of (*E*)-**1a** with light of a wavelength of 366 nm triggers a tenfold rate enhancement of the coupling reaction. The template effects of the *E* isomers (*E*)-**1a,b** correlate well with the results of our binding studies. The more extended template (*E*)-**1b**, which was unable simultaneously to coordinate the two adenine functionalities of **4** also lacks the complementary surface to the transition state of the reaction. In fact binding of the two substrates **2** and **3** at a remote distance slows down the reaction. On the other hand, the less extended template (*E*)-**1a** slightly accelerates the reaction. The capability to fold to a conformation, which is complementary to product **4** (previous binding studies), obviously also enables accommodation of the species along the reaction coordinate. However, the conformations demanded to

Table 3 Effect of one equivalent of template **1a,b** at different *E*/*Z* ratios on the initial rate of the coupling reaction between **2** and **3**

Receptor	*E*/*Z* ratio	Additive (equiv.)[a]	Acceleration[b]
1a	100/0	—	1.2
1a	70/30	—	6.3
1a	50/50	—	10.5
1a	50/50	**11** (10)	1.9
1a	50/50	**4** (1)	1.7
1b	100/0	—	0.8
1b	50/50	—	2.5

[a] Equivalents of added competitive binders. [b] Increase of the initial rate compared with the uncatalysed reaction with $k = 1.5 \times 10^{-8}$ dm^3 mol^{-1} min^{-1} [ref. 9(*a*)]; the standard deviations are less than 10%.

enable coupling are not favourable for this template and the efficiency of the template is therefore marginal. On the contrary, catalytic activity is observed after switching the templates into their photostationary equilibria at 366 nm. (*Z*)-**1a** accelerates the reaction considerably to the observed 20-fold for the pure *Z* isomer.

Typical features expected for a template-directed reaction involving a termolecular complex are product inhibition and inhibition by competitive binders. Both effects are observed as shown for **4** and **11**. Bis-adenine **4** exerts the bigger effect which again reflects the higher binding affinity for this guest molecule. Molecular modelling[12] suggests several conformations for the termolecular complexes (*Z*)-**1a**·**2**·**3** and (*Z*)-**1b**·**2**·**3** that provide access to the tetrahedral intermediate and also to product **4**. Of course, as a consequence of the flexibility of both receptors **1a,b** there are also a lot of unfavourable conformations. For this reason we are unable to account for the different activity of (*Z*)-**1a** and (*Z*)-**1b**. It is tempting, however, to assume that receptor (*Z*)-**1a** is more active because it exists with a higher probability in a productive conformation than does receptor (*Z*)-**1b**.[9b,c]

On the basis of our binding studies it is possible to calculate the intrinsic efficiency§ of the receptors. Assuming averaged adenine–receptor binding constants of 35 500 dm^3 mol^{-1} and independent binding events at the two binding sites for both receptors (*E*)-**1a** and (*Z*)-**1a** (which is in accordance with the data in Table 2) an initial amount of 17% of termolecular complex **1**·**2**·**3** is calculated. With this value and the observed 10.5-fold rate acceleration a corrected accelerating factor of 110-fold is obtained for (*Z*)-**1a**. Similarly an accelerating factor of about two-fold can be estimated for (*E*)-**1a**. Therefore the intrinsic catalytic activity of the two interswitchable structures (*E*)-**1a** and (*Z*)-**1a** varies by a factor of about 50.

Influence of adenine guest molecules on the thermal *Z* ⟶ *E* isomerization

The results of the last section suggest that bis-adenine **4** is strongly chelated by the two receptors of (*Z*)-**1a,b**. As the thermal *Z* ⟶ *E* isomerization demands removal of at least one adenine from its receptor site, an inhibition of this isomerization process by **4** is expected (Fig. 6).

Such a suppression of a *Z*/*E* isomerization process has been observed by Shinkai *et al.* for crown-ether functionalized azobenzenes when the appropriate metal cations were added as a guest.[19] Another interesting example of an isomerization process of a cryptand-type crown spirobenzopyran which was *induced* by binding of a metal ion guest was described recently.[20]

§ The term intrinsic efficiency is used to describe the corrected acceleration for the reaction within the termolecular complex. On the basis of the unproductive template (*E*)-**1b**, the rate of the background reaction that still occurs in the presence of templates was assumed to be 0.8 times that of the original background reaction (without added receptor molecules). The relative reaction rate originating from the 17% **2** and **3** assembled in a termolecular complex (*E*)-**1a**·**2**·**3** [but only 8.5% (*Z*)-**1a**·**2**·**3**] is then 9.7-fold for (*Z*)-**1a** and 0.4-fold for (*E*)-**1a**. This corresponds to a corrected acceleration factor of 110- and 2-fold for the rate of the reaction within the termolecular complex.[18]

Table 4 Rate constants $k/10^{-5}$ min^{-1} of the thermal *Z* ⟶ *E*-isomerization in chloroform at 25 °C in the absence and in the presence of adenine derivatives (1 equivalent/binding site)[a]

Additive	(*Z*)-**1a**[b]	(*Z*)-**1b**	(*Z*)-**9a**	(*Z*)-**9b**
—	8	7	10	23
11	14	13	11	23
2	17	12	—	—
4	6	4	10	23

[a] Determined by UV–VIS spectroscopy of 0.05 mmol dm^{-3} solutions; error ± 10%. [b] Determined at 40 °C; at 25 °C the rate is too slow for an accurate evaluation [$k < 1 \times 10^{-5}$ min^{-1} for pure (*Z*)-**1a** at 25 °C].

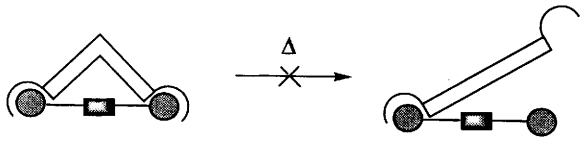

Fig. 6 Schematic illustration of the inhibition of the *Z* ⟶ *E* isomerization by ditopic complexation

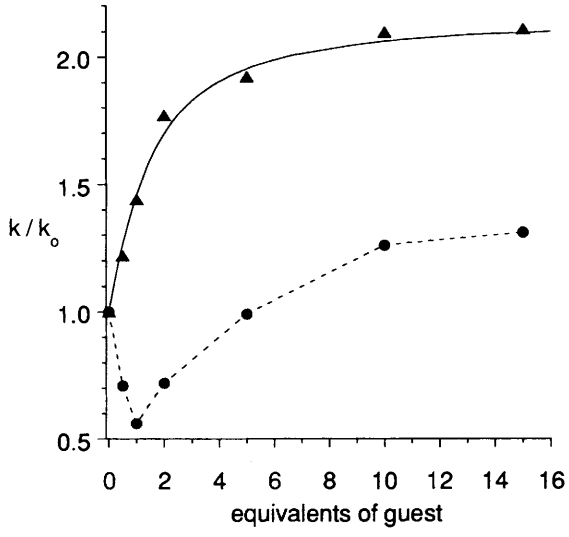

Fig. 7 Dependence of the thermal *Z* ⟶ *E* isomerization rate *k* of receptor (*Z*)-**1b** on the amount of added guest **11** (▲) and **4** (●) in chloroform (0.05 mmol dm^{-3}; 25 °C; $k_0 = 7 \times 10^{-5}$ min^{-1})

Table 4 gives the rate constants for the thermal *Z* ⟶ *E* isomerization of (*Z*)-**1a,b** and the model compounds (*Z*)-**9a,b** in the presence of stoichiometric amounts of adenine compounds. The dependence of the *Z* ⟶ *E* isomerization of (*Z*)-**1b** on the concentration of 9-ethyladenine and product **4** is shown in Fig. 7.

It follows from Table 4 and Fig. 7 that at least two effects by adenine binding are involved. (1) The addition of mono-adenine derivatives causes a rate increase for the *Z* ⟶ *E* isomerization of (*Z*)-**1a,b**. That this effect is related to adenine binding to the receptor site is demonstrated by the binding isotherm shown in the figure (solid line, calculated for $K = 20\,000$ dm^3 mol^{-1})¶ and by the fact that no influence of adenines on the *Z* ⟶ *E* conversion of **9a,b** is observed. (2) The addition of one equivalent of product **4** causes a rate decrease for the *Z* ⟶ *E*

¶ As it is difficult to make reasonable assumptions on the exact dependence of the rate on the first and the second adenine binding event, a simple 1:1 model was applied. The value of 20 000 dm^3 mol^{-1} is therefore just to show the order of magnitude.

isomerization of (*Z*)-**1a,b**. This effect is reversed at higher concentrations of **4**.

The former influence of adenines on the isomerization process and the (in general) slower isomerization of receptors (*Z*)-**1a,b** compared with (*Z*)-**9a,b** are difficult to explain. Aggregation of the receptors or intramolecular self-association by the imide functionalities might slow the isomerization of these receptors (*Z*)-**1a,b** when adenines are absent. On the other hand, electronic or steric effects of the coordinated adenines on the (*Z*)-azobenzene subunit might account for an increased isomerization rate.

More interesting is the dependence of the $Z \longrightarrow E$ isomerization rate on the concentration of product **4**. By merely looking at the first three data points (< 1 equivalent) a mirror image of the curve obtained for **11** might be expected with an asymptotic value close to zero. However, at higher concentrations of **4** (> 1 equivalent) the curve turns in the opposite direction and now follows the one for **11**, but with a lower asymptotic value. To explain these observations we have to recapitulate the results of our binding studies. Whereas the first binding event of an adenine derivative to receptors **1a,b** yields an association energy of about 6–7 kcal mol^{-1}, the second binding event is only weak, contributing about 1–2 kcal mol^{-1} to the total binding energy. Therefore it seems very likely that at higher concentrations of **4** the second adenine group is substituted by another molecule **4** to give a 1:2 complex. Although the $Z \longrightarrow E$ isomerization rate increases with the formation of a 1:2 complex, the asymptotic value remains clearly below that observed for **11**. Presumably this difference is caused by some stabilizing van der Waals interaction between the larger molecule **4** and the (*Z*)-azobenzene subunit, which is not possible for the smaller adenine derivatives. Thus, besides showing the influence of substrate binding on the reactivity of the azobenzenes (*Z*)-**1a,b** we were able to gain information on the stoichiometry of the complexes between (*Z*)-**1a,b** and **4**, which was not available by UV–VIS titration.

Conclusions

The present study establishes (*a*) that a combination of subunits for recognition, reactivity and photocontrol in a supramolecular assembly affords photoresponsive receptors **1a,b**, wherein all functional units work in the expected way, (*b*) the rate of the geometrical isomerization of the (*Z*)-azobenzene unit is affected by organic guest molecules (adenines) and, especially, (*c*) that photoswitchable receptor molecules **1a,b** are capable of controlling a coupling reaction between two adenine substrate molecules *via* formation of a termolecular complex. Thus for the more efficient template **1a** $E \longrightarrow Z$ switching triggers a 50-fold increase in the template's catalytic activity. As the release of the product **4** is facilitated by photoswitching templates (*Z*)-**1a,b** back to the *E* form, the incorporation of photoresponsive components might offer a strategy to achieve turnover in template systems.

Experimental

^{1}H NMR spectra were obtained with a Varian XL-300 instrument at 300 MHz; chemical shifts and coupling constants (*J*) are given in δ-values (ppm) and in hertz (Hz), respectively. UV–VIS absorption measurements were taken on a Perkin-Elmer Lambda 2 spectrophotometer equipped with a 6 cell changer system, a thermostat and a PC with the Perkin-Elmer software package PECSS, version 4.2. High resolution mass spectra were obtained with a Finnigan Mat 8200 instrument in the fast atom bombardment mode (mNBA matrix). The parent molecular ions invariably formed the most intense peaks and the isotope pattern was consistent with $M^{\cdot+}$ and $[M + H]^+$ as the main ions. For molecules with more than 90 carbons the presence of one ^{13}C molecule was considered in the calculated mass. Melting points were determined on an Electrothermal 9100 melting point apparatus.

All commercially available compounds were used without further purification unless otherwise indicated. THF was distilled from sodium; pyridine was stirred for one day over potassium hydroxide, filtered and distilled. The chloroform used for the spectrophotometric studies was obtained from J. T. Baker (Baker Analyzed HPLC reagent) and stored over 4 Å molecular sieves. Analytical TLC was performed on Merck precoated 0.2 mm plates of silica gel 60 F_{254}.

Photoisomerization

The photoisomerization was performed by irradiation of 0.05–2 mmol solutions of (*E*)-**1a,b** or (*E*)-**9a,b** in chloroform, or deuteriated chloroform for the NMR studies. For UV irradiation a 4 W UVP UVGL-25 lamp was used (longwave UV tube: 366 nm). The photostationary equilibrium was obtained after 5 min–2 h, depending on the compound and the concentration of the solution. Visible light irradiation was performed with a 500 W tungsten lamp. UV–VIS spectra were taken for each photostationary equilibrium. The *E*/*Z* ratio was determined by ^{1}H NMR spectroscopy.

Binding studies by UV titrations

Titrations were performed at 0.01 mol dm^{-3} constant host concentration in chloroform at room temperature. Two 1 cm quartz cuvettes with 700 μl 0.01 mmol dm^{-3} host solution and 700 μl pure chloroform were placed in a double beam spectrophotometer. Guest solutions of 0.05 mmol dm^{-3} **4** (or 0.1 mmol dm^{-3} **11**) were prepared in 0.01 mmol dm^{-3} host solution and in pure chloroform. Aliquots of these solutions were placed in the cuvette with the host solution and in the reference cuvette, respectively (10 μl at first, then 25 μl and finally 50 μl) and a spectrum was recorded after each addition. The addition of guest was continued until saturation was reached. The association constants were determined by non-linear least-squares regression analysis[21] from the absorbance change at 313 nm.

Kinetics of the amide bond formation

In a 1 cm quartz cuvette chloroform solutions of amine **2** (125 μl; 0.4 mmol dm^{-3}), triethylamine (125 μl; 32 mmol dm^{-3}), eventually inhibitor **4** or **11** (125 μl; 0.4 mmol dm^{-3}, resp.) and template (125 μl; 0.4 mmol dm^{-3}) were mixed together and the volume was adjusted to 875 cm^3 with chloroform. A solution of active ester **3** (125 μl, 0.4 mmol dm^{-3}) was added and the solution was shaken and transferred to the temperature-controlled (25 ± 0.1 °C) compartment of the spectrometer. The reaction was monitored at 380 or 390 nm to about 60% completion by following the release of *p*-nitrophenolate. Reactions were run with and without amine **2** to ensure that *p*-nitrophenolate release was due to aminolysis rather than hydrolysis and that thermal $Z \longrightarrow E$ isomerization of azobenzene was negligible. Initial rates were determined from the first 10% of the reaction. Reactions were run at least in duplicate and the numbers were averaged. The UV evaluation method was confirmed by ^{1}H NMR analysis of an 80% completed reaction.[9]

$Z \longrightarrow E$ isomerization studies

(*E*)-azobenzenes were converted into their photostationary equilibria at 366 nm and 0.05 mmol dm^{-3} solutions containing the desired amount of adenine additive were prepared as described above in a quartz cuvette. The isomerization reactions were monitored at 25 °C (and at 40 °C for **1a**) for 20 h at several

wavelengths between 330 nm and 360 nm. Reactions were run at least in triplicate and the numbers were averaged. First-order rate constants k were calculated from the slope of the linear plots of $\ln[A_0 - A(t)]$ against time (A_0: absorbance of pure (*E*)-azobenzene at 0.05 mmol dm^{-3}).

Molecular modelling

All molecular modelling was performed on a Silicon Graphics 4D30G + Personel Iris with Macromodel 3.5X.[12] Possible conformations for the complexes **1·2·3**, **1·4** and of **1** with the assumed tetrahedral intermediate were derived by minimization using the truncated Newton conjugate gradient (TCNG)[22] and a modified Amber force field.

3,6-Diaminocarbazole

3,6-Dinitrocarbazole (3 g, 11.7 mmol) was suspended in 240 cm^3 THF and hydrogenated at balloon pressure for 4 days with 5% palladium-on-carbon (150 mg). The solid was filtered off and extracted for 24 h in a Soxhlet apparatus with methanol–THF (1 : 1). The combined filtrates were collected and evaporated to give a grey solid, which was washed with ethanol to remove the dark polar impurities. A white solid was obtained which was washed with a little ether and dried to give pure 3,6-diaminocarbazole (2.09 g, 91%), mp > 300 °C (lit.,[23] 320–322 °C); δ_H[$(CD_3)_2SO$] 10.1 (1 H, s, NH), 7.05 (4 H, m, 1-H, 4-H, 5-H, 8-H), 6.65 (2 H, dd, *J* 8.3, *J* 1.8, 2-H, 7-H) and 4.6 (4 H, br s, NH_2).

3,6-Diphthalimidocarbazole 5

3,6-Diaminocarbazole (0.23 g, 1.167 mmol) was dissolved in 40 cm^3 dry pyridine under argon and phthaloyl dichloride (0.50 g, 2.45 mmol) was added dropwise by syringe whereupon the solution turned dark red. The solution was heated to reflux to become bright orange. After reflux for 6 h the pyridine was evaporated off and the crude product was washed with ether and purified by chromatography on silica gel with dichloromethane–methanol (95 : 5) to give compound **5** as a yellow solid (0.52 g, 97%), mp > 300 °C; ν_{max}(KBr)/cm^{-1} 3390, 1711, 1498, 1469, 1385, 1246, 1112, 1083 and 719; δ_H[$(CD_3)_2SO$] 11.7 (1 H, s, NH), 8.17 (2 H, d, *J* 1.4, carb. 4-H, 5-H), 7.90–8.00 (8 H, $m_{AA'BB'}$, phthalimide 3-H, 4-H, 5-H, 6-H), 7.66 (2 H, d, *J* 8.5, carb. 1-H, 8-H) and 7.47 (2 H, dd, *J* 8.5, *J* 1.6, carb. 2-H, 7-H); HRMS (FAB) *m*/*z* calc. for $C_{28}H_{16}N_3O_4$ [$(M + H)^+$] 458.114 08, found 458.114 47.

(*E*)-4,4′-Bis[(3,6-diphthalimidocarbazol-9-yl)methyl]-azobenzene (*E*)-7b

Under argon phthalimidocarbazole **5** (0.30 g, 0.66 mmol) and 18-crown-6 (0.026 g, 0.1 mmol) were dissolved in 30 cm^3 of dry THF and 0.7 cm^3 of a 1 mol dm^{-3} solution of potassium *tert*-butoxide in THF (0.7 mmol) was added by syringe. The colour changed from yellow to orange-red and a brown precipitate formed. Azo compound (*E*)-**6b** (0.11 g, 0.30 mmol) was dissolved in 30 cm^3 hot THF and slowly added *via* a dropping funnel. The suspension was stirred for 8 h at room temperature. The precipitate was filtered off and washed with 30 cm^3 THF. The combined filtrates were evaporated to 2–3 cm^3 and the precipitation was completed by adding about 30 cm^3 of ether. The solid was washed with ether and *n*-pentane and the crude product (250 mg) was purified by chromatography on silica gel with dichloromethane–methanol (95 : 5) to give (*E*)-**7b** as a yellow solid (0.14 g, 42%), mp > 300 °C; ν_{max}(KBr)/cm^{-1} 1714, 1494, 1474, 1374, 1220, 1111, 1081 and 716; δ_H[$(CD_3)_2SO$] 8.25 (4 H, d, *J* 1.8, carb. 4-H, 5-H), 7.90–8.00 (16 H, $m_{AA'BB'}$, phthalimide 3-H, 4-H, 5-H, 6-H), 7.82 (8 H, m, carb. 1-H, 8-H, azobenz. 2-H, 6-H), 7.54 (4 H, dd, *J* 8.6, *J* 1.8, carb. 2-H, 7-H), 7.41 (4 H, d, *J* 8.5, azobenz. 3-H, 5-H) and 5.90 (4 H, br s, CH_2); HRMS (FAB) *m*/*z* calc. for $C_{70}H_{41}N_8O_8$ [$(M + H)^+$] 1121.3047, found 1121.3002.

(*E*)-3,3′Bis[(3,6-diphthalimidocarbazol-9-yl)methyl]-azobenzene (*E*)-7a

As described for (*E*)-**7b** from **5** (0.30 g, 0.66 mmol), azo compound (*E*)-**6a** (0.11 g, 0.30 mmol), in 1 cm^3 of 1 mol dm^{-3} potassium *tert*-butoxide in THF and 18-crown-6 (0.026 g, 0.1 mmol) in 60 cm^3 dry THF to give (*E*)-**7a** as a yellow-orange solid (0.134 g, 40%), mp > 300 °C; ν_{max}(KBr)/cm^{-1} 1715, 1495, 1474, 1373, 1111, 1081 and 715; δ_H[$(CD_3)_2SO$] 8.25 (4 H, d, *J* 1.9, carb. 4-H, 5-H), 7.8–8.0 (16 H, $m_{AA'BB'}$, phthalimide 3-H, 4-H, 5-H, 6-H), 7.87 (4 H, d, *J* 8.9, carb. 1-H, 8-H), 7.83 (2 H, m, azobenz. 2-H), 7.75 (2 H, br d, *J* 8, azobenz. 6-H), 7.55 (4 H, dd, *J* 8.7, *J* 2.0, carb. 2-H, 7-H), 7.50 (2 H, t, *J*, 8.5, azobenz. 5-H) and 7.34 (2 H, br, d, *J* 7, azobenz. 4-H); HRMS (FAB) *m*/*z* calc. for $C_{70}H_{41}N_8O_8$ [$(M + H)^+$] 1121.3047, found 1121.3002.

4,4′-Azobenzene-bis-receptor 1b

Phthaloyl-protected tetraamine (*E*)-**7b** (45 mg, 0.040 mmol) was suspended in 30 cm^3 THF–methanol (1 : 1) and 2 cm^3 of a 40% solution of methylamine in water was added. After stirring for 10 h, the solution was evaporated to about 2 cm^3 and precipitation was completed by addition of 20 cm^3 of ether. The yellow-orange solid was filtered off and washed with ether and pentane. After drying, 21 mg (87%) of crude tetraamine were obtained which were used for acylation.

A small fraction of pure (E)-4,4′-*bis*[(3,6-*diaminocarbazol*-9-*yl*)*methyl*]*azobenzene* was isolated by chromatography on basic aluminium oxide III with dichloromethane–methanol (90 : 10); δ_H[$(CD_3)_2CO$] 7.71 (4 H, *J* 8.3, azobenz. 2-H, 6-H), 7.24 (4 H, d, *J* 8.5, azobenz. 3-H, 5-H), 7.20 (4 H, d, *J* 8.5, carb. 1-H, 8-H), 7.15 (4 H, d, *J* 2.1, carb. 4-H, 5-H), 6.72 (4 H, dd, *J* 8.5, *J* 2.1, carb. 2-H, 7-H), 5.49 (4 H, s, CH_2) and 5.0 (8 H, s, NH_2); HRMS (FAB) *m*/*z* calc. for $C_{38}H_{33}N_8$ [$(M + H)^+$] 601.282 82, found 601.282 72.

Crude tetraamine (18 mg, 0.030 mmol) and imide acid chloride **8** (50 mg, 0.143 mmol) were dissolved in 6 cm^3 dry pyridine and the solution was heated to reflux for 6 h under argon in the dark. Under exclusion of light the pyridine was evaporated off, the yellow solid was dissolved in 25 cm^3 dichloromethane and the organic layer was washed with 1 mol dm^{-3} HCl, 1 mol dm^{-3} $NaHCO_3$ and water and dried over Na_2SO_4. After chromatography on silica gel with dichloromethane–methanol (98 : 2) (*E*)-**1b** was obtained as a yellow solid [36 mg, 58% based on (*E*)-**7b**], mp 243–247 °C; λ_{max}($CDCl_3$)/nm 290 (ε/dm^3 mol^{-1} cm^{-1} 60 000), 332 (30 200) and 438sh (1020); ν_{max}(KBr)/cm^{-1} 3450, 3379, 2958, 2932, 2871, 1700, 1490, 1467, 1308, 1196 and 802; δ_H[$(CD_3)_2CO$] 9.2 (4 H, br s, imide NH), 8.6 (4 H, s, amide NH), 8.16 (4 H, d, *J* 1.8, carb. 4-H, 5-H), 7.79 (4 H, d, *J* 8.5, azobenz. 2-H, 6-H) 7.54 (4 H, dd, *J* 8.8, *J* 1.9, carb. 2-H, 7-H), 7.39 (4 H, d, *J* 8.8, carb. 1-H, 8-H), 7.33 (4 H, d, *J* 8.6, azobenz. 3-H, 5-H), 5.68 (4 H, s, CH_2), 2.78 (8 H, d, *J* 12, cyclohexyl), 2.20 (4 H, d, *J* 12, cyclohexyl), 1.91 (8 H, m, cyclohexyl), 1.59 (8 H, m), 1.2–1.5 (44 H, m) and 0.90 (36 H, m, CH_3); HRMS (FAB) *m*/*z* calc. for $C_{110}H_{140}N_{12}O_{12}$ ($M^{\cdot+}$) 1822.0747, found 1822.0697.

(*Z*)-**1b** was obtained by irradiation at 366 nm in form of a 1 : 1 mixture with the *E* isomer, λ_{max}($CHCl_3$) for (*E*)/(*Z*)-**1b** (1 : 1)/nm 289 (ε/dm^3 mol^{-1} cm^{-1} 65 000), 322 (16 300) and 438 (1530); δ_H[$(CD_3)_2CO$] 9.3 (4 H, br s, imide NH), 8.7 (4 H, br s, amide NH), 8.07 (4 H, br s, carb. 4-H, 5-H), 7.59 (4 H, dd, *J* 8.8, *J* 1.8, carb. 2-H, 7-H), 7.27 (4 H, d, *J* 8.8, carb. 1-H, 8-H), 6.96 (4 H, d, *J* 8.2, azobenz.), 6.65 (4 H, d, *J* 8.4, azobenz.), 5.50 (4 H, s, CH_2) and aliphatic protons as for (*E*)-**1b**.

3,3′-Azobenzene-bis-receptor 1a

As described above for **1b** phthaloyl-protected tetraamine (*E*)-

7a (85 mg, 0.076 mmol) was deprotected by methylamine (5 cm^3 40% solution in water) in 50 cm^3 THF–methanol and the crude tetraamine (45 mg) was acylated with imide acid chloride **8** (155 mg, 0.44 mmol) in 10 cm^3 pyridine to give, after work-up and chromatography under exclusion of light, (*E*)-**1a** as a yellow solid (78 mg, 56%), mp 227–230 °C; $\lambda_{max}(CHCl_3)$/nm 289 (ε/dm^3 mol^{-1} cm^{-1} 65 000), 330sh (23 000) and 439 (670); ν_{max}(KBr)/cm^{-1} 3448, 3378, 2958, 2872, 1700, 1466, 1400, 1308, 1197 and 802; $\delta_H[(CD_3)_2CO]$ 9.3 (4 H, s, imide NH), 8.6 (4 H, s, amide NH), 8.14 (4 H, s, carb. 4-H, 5-H), 7.69 (4 H, m, azobenz. 2-H, 6-H), 7.57 (4 H, dd, *J* 8.7, *J* 1.8, carb. 2-H, 7-H), 7.4–7.5 (6 H, m, carb. 1-H, 8-H, azobenz. 5-H), 7.29 (2 H, d, *J* 7.7, azobenz. 4-H), 5.66 (4 H, s, CH_2), 2.81 (8 H, d, *J* 12, cyclohexyl), 2.21 (4 H, d, *J* 12, cyclohexyl), 1.93 (8 H, m, cyclohexyl), 1.62 (8 H, m), 1.2–1.5 (44 H, m) and 0.9 (36 H, m, CH_3). At room temp. all peaks were rather broad. By increasing the temperature to 40 °C sharp and better-resolved peaks were observed; HRMS (FAB) *m*/*z* calc. for $C_{110}H_{140}N_{12}O_{12}$ ($M^{\cdot+}$) 1822.0747, found 1822.0697.

(*Z*)-**1a** was obtained by irradiation at 366 nm in the form of a 1 : 1 mixture with the *E* isomer, $\lambda_{max}(CHCl_3)$ for (*E*)/(*Z*)-**1a** (1 : 1)/nm 289 (ε/dm^3 mol^{-1} cm^{-1} 64 000), 330sh (13 400) and 437 (950); $\delta_H[(CD_3)_2CO]$ 9.2 (4 H, s, imide NH), 8.6 (4 H, s, amide NH), 8.08 (4 H, s, carb. 4-H, 5-H), 7.43 (4 H, m, carb. 2-H, 7-H), 7.15 (4 H, d, azobenz. 4-H, 5-H), 6.96 (4 H, d, *J* 8.8, carb. 1-H, 8-H), 6.64 (2 H, m, azobenz. 6-H), 5.87 (2 H, s, azobenz. 2-H), 5.16 (4 H, s, CH_2) and aliphatic part as for (*E*)-**1a**; At room temp. all peaks were rather broad. By increasing the temperature to 40 °C sharp and better-resolved peaks were observed.

Acknowledgements

We thank the National Institutes of Health for supporting this research, and the Alexander von Humboldt Foundation for a Feodor Lynen Fellowship to F. W.

References

1 J.-M. Lehn, *Angew. Chem.*, 1988, **100**, 91–116; *Angew. Chem., Int. Ed. Engl.*, 1988, **27**, 89–112; J.-M. Lehn, *Angew. Chem.*, 1990, **102**, 1347–1362; *Angew. Chem., Int. Ed. Engl.*, 1990, **29**, 1304–1319; V. Balzani and F. Scandola, *Supramolecular Photochemistry*, Ellis Horwood, Chichester, 1991.

2 J.-P. Behr and J.-M. Lehn, *J. Am. Chem. Soc.*, 1973, **95**, 6108–6110; J. L. Sessler, H. Furuta and V. Král, *Supramol. Chem.*, 1993, **1**, 209–220; L. K. Mohler and A. W. Czarnik, *J. Am. Chem. Soc.*, 1993, **115**, 7073–7038; P. R. Westmark and B. D. Smith, *J. Am. Chem. Soc.*, 1994, **116**, 9343–9344; M. T. Reetz, J. Huff, J. Rudolph, K. Töllner, A. Deege and R. Goddard, *J. Am. Chem. Soc.*, 1994, **116**, 11588–11589; E. G. Reichwein-Buitenhuis, H. C. Visser, F. de Jong and D. N. Reinhoudt, *J. Am. Chem. Soc.*, 1995, **117**, 3913–3921; C. Andreu, A. Galán, K. Kobiro, J. de Mendoza, T. K. Park, J. Rebek, Jr., A. Salmerón and N. Usman, *J. Am. Chem. Soc.*, 1994, **116**, 5501–5502.

3 H.-G. Löhr and F. Vögtle, *Acc. Chem. Res.*, 1985, **18**, 65–72; R. C. Helgeson, B. P. Czech, E. Chapoteau, C. R. Gebauer, A. Kumar and D. J. Cram, *J. Am. Chem. Soc.*, 1989, **111**, 6339–6350; R. A. Bissell, A. P. de Silva, H. Q. N. Gunaratne, P. L. M. Lynch, G. E. M. Maguire and K. R. A. S. Sandanayake, *Chem. Soc. Rev.*, 1992, **21**, 187–195; A. W. Czarnik, *Acc. Chem. Res.*, 1994, **27**, 302–308; P. D. Beer, *Adv. Mater.*, 1994, **6**, 607–609; M. Inouye, K. Hashimoto and K. Isagowa, *J. Am. Chem. Soc.*, 1994, **116**, 5517–5518; R. Grigg, J. M. Holmes, S. K. Jones and W. D. J. A. Norbert, *J. Chem. Soc., Chem. Commun.*, 1994, 185–187; K. R. A. S. Sandanayake and S. Shinkai, *J. Chem. Soc., Chem. Commun.*, 1994, 1083–1084.

4 S. Anderson, H. L. Anderson and J. K. M. Sanders, *Acc. Chem. Res.*, 1993, **26**, 469–475; R. Hoss and F. Vögtle, *Angew. Chem.*, 1994, **106**, 389–398; *Angew. Chem., Int. Ed. Engl.*, 1994, **33**, 375–384; T. R. Kelly, G. J. Bridger and C. Zhao, *J. Am. Chem. Soc.*, 1990, **112**, 8024–8034; D. Sievers and G. von Kiedrowski, *Nature (London)*, 1994, **369**, 221–224; J. Rebek, Jr., *Chem. Br.*, 1994, **30**, 286–290.

5 I. Willner and B. Willner in *Bioorganic Photochemistry, Vol. 2: Biological Applications of Photochemical Switches*, ed. H. Morrison, Wiley, New York, 1993, pp. 1–110; S. Shinkai and O. Manabe, *Top. Curr. Chem.*, 1984, **121**, 67–104 and references cited therein; H.-W. Losensky, H. Spelthann, A. Ehlen, F. Vögtle and J. Bargon, *Angew. Chem.*, 1988, **100**, 1225–1227; *Angew. Chem., Int. Ed. Engl.*, 1988, **27**, 1189–1191; I. Willner, S. Marx and Y. Eichen, *Angew. Chem.*, 1992, **104**, 1255–1257; *Angew. Chem., Int. Ed. Engl.*, 1992, **31**, 1243–1244; T. Hohsaka, K. Kawashima and M. Sisido, *J. Am. Chem. Soc.*, 1994, **116**, 413–414; M. Lion-Dagan, E. Katz and I. Willner, *J. Am. Chem. Soc.*, 1994, **116**, 7913–7914; R. A. Bisell, E. Córdova, A. E. Kaifer and J. F. Stoddart, *Nature (London)*, 1994, **369**, 133–137; P. R. Ashton, R. Ballardini, V. Balzani, M. T. Gandolfi, D. J.-F. Marquis, L. Pérez-Garcia, L. Prodi, J. F. Stoddard and M. Venturi, *J. Chem. Soc., Chem. Commun.*, 1994, 177–180; T. Nabeshima, H. Furusawa and Y. Yano, *Angew. Chem.*, 1994, **106**, 1849–1851; *Angew. Chem., Int. Ed. Engl.*, 1994, **33**, 1750–1751; A. Livoreil, C. O. Dietrich-Buchecker and J.-P. Sauvage, *J. Am. Chem. Soc.*, 1994, **116**, 9399–9400; M. Bauer, W. M. Müller, U. Müller, K. Rissanen and F. Vögtle, *Liebigs Ann. Chem.*, 1995, 649–656.

6 A portion of this work appeared in a preliminary communication: F. Würthner and J. Rebek, Jr., *Angew. Chem.*, 1995, **107**, 503–505; *Angew. Chem., Int. Ed. Engl.*, 1995, **34**, 446–448.

7 L. Stryer, *Annu. Rev. Neurosci.*, 1986, **9**, 87–119; P. A. Liebman, K. R. Parker and E. A. Dratz, *Ann. Rev. Physiol.*, 1987, **49**, 765–791; F. Siebert in *Photochromism, Molecules and Systems*, eds. H. Dürr and H. Bouas-Laurent, Elsevier, Amsterdam, 1990, pp. 756–792.

8 (*a*) M. M. Conn, G. Deslongchamps, J. de Mendoza and J. Rebek, Jr., *J. Am. Chem. Soc.*, 1993, **115**, 3548–3557; (*b*) R. J. Pieters and J. Rebek, Jr., *Recl. Trav. Chim. Pays-Bas*, 1993, **112**, 330–334.

9 (*a*) R. J. Pieters, I. Huc and J. Rebek, Jr., *Tetrahedron*, 1995, **51**, 485–498; (*b*) I. Huc, R. J. Pieters and J. Rebek, Jr., *J. Am. Chem. Soc.*, 1994, **116**, 10296–10297; (*c*) R. J. Pieters, I. Huc and J. Rebek, Jr., *Chem. Eur. J.*, 1995, **1**, 223–232.

10 H. Rau, *Angew. Chem.*, 1973, **85**, 248–258; *Angew. Chem., Int. Ed. Engl.*, 1973, **12**, 224–235; H. Rau in *Photochromism, Molecules and Systems*, eds. H. Dürr and H. Bouas-Laurent, Elsevier, Amsterdam, 1990, pp. 165–192; J. Griffiths, *Chem. Soc. Rev.*, 1972, **1**, 481–493.

11 R. Allmann in *The Chemistry of the Hydrazo, Azo and Azoxy Groups*, Part 1, ed. S. Patai, Wiley, New York, 1975, pp. 23–52.

12 (*a*) F. Mohamadi, N. G. Richards, W. C. Guida, R. Liskamp, M. Lipton, C. Caufield, G. Chang, T. Hendrickson and W. C. Still, *J. Comput. Chem.*, 1990, **11**, 440–467; (*b*) W. C. Still, A. Tempczyk, R. C. Hawley and T. Hendrickson, *J. Am. Chem. Soc.*, 1990, **112**, 6127–6129.

13 (*a*) E. Bartels, N. H. Wassermann and B. F. Erlanger, *Proc. Nat. Acad. Sci. USA*, 1971, **68**, 1820–1823; (*b*) N. H. Wassermann and B. F. Erlanger, *Chem.-Biol. Interact.*, 1981, **36**, 251–258.

14 K. S. Jeong, T. Tjivikua, A. Muehldorf, G. Deslongchamps, M. Famulok and J. Rebek, Jr., *J. Am. Chem. Soc.*, 1991, **113**, 201–209.

15 P. P. Birnbaum, J. H. Linford and D. W. G. Style, *Trans. Faraday Soc.*, 1953, **49**, 735–744; H. Bisle, M. Römer and H. Rau, *Ber. Bunsenges. Phys. Chem.*, 1976, **80**, 301–305.

16 For a discussion of different mechanisms of energy transfer see: N. J. Turro, *Molecular Photochemistry*, W. A. Benjamin, London, 1965.

17 (*a*) K. A. Connors, *Binding Constants*, 1st edn., Wiley, New York, 1987; (*b*) C. S. Wilcox in *Frontiers in Supramolecular Organic Chemistry and Photochemistry*, eds. H. J. Schneider and H. Dürr, VCH, Weinheim, 1991, pp. 123–143.

18 For an alternative description based on effective molarity see: M. I. Page, *Angew. Chem.*, 1977, **89**, 456–467; *Angew. Chem., Int. Ed. Engl.*, 1977, **16**, 449–459.

19 S. Shinkai, T. Nakaji, Y. Nishida, T. Ogawa and O. Manabe, *J. Am. Chem. Soc.*, 1980, **102**, 5860–5865.

20 M. Inouye, Y. Noguchi and K. Isagawa, *Angew. Chem.*, 1994, **106**, 1226–1228; *Angew. Chem., Int. Ed. Engl.*, 1994, **33**, 1163–1166.

21 Systat 5.2., Systat Inc.; Evanston, IL, 1992.

22 J. W. Ponder and F. M. Richards, *J. Comput. Chem.*, 1987, **8**, 1016–1024.

23 H. M. Grotta, C. J. Riggle and A. E. Bearse, *J. Org. Chem.*, 1964, **29**, 2474–2476.

Paper 5/03376D
Received 25*th May* 1995
Accepted 15*th June* 1995